$$x' = \begin{pmatrix} * & * & * \\ * & * & * \\ 0 & 0 & * \end{pmatrix} x + \begin{pmatrix} * & 0 \\ 0 & * \\ 0 & 0 \end{pmatrix} \begin{pmatrix} u_1(t) \\ u_2(t) \end{pmatrix}$$

where $*$ stands for an arbitrary t-dependent entry which is $(d-2)$ and $(d-1)$ times continuously differentiable, respectively.

The next simple example shows that Theorem 2.1 makes a more refined statement about noncontrollability if the structure of the matrix A is known in more detail.

Example 3.2: Consider the control system

$$x' = \begin{pmatrix} a(t) & 1 & 2 \\ 1 & 4 & 2 \\ 2 & 2 & 7 \end{pmatrix} x + \begin{pmatrix} 1 \\ 0 \\ 0 \end{pmatrix} u(t).$$

Although this system is not of one of the types given in Example 3.1, our Theorem 2.1 yields with

$$A_1 = \begin{pmatrix} 1 & 0 & 0 \\ 0 & 0 & 0 \\ 0 & 0 & 0 \end{pmatrix} \quad A_2 = \begin{pmatrix} 0 & 1 & 2 \\ 1 & 4 & 2 \\ 2 & 2 & 7 \end{pmatrix} \quad B = \begin{pmatrix} 1 \\ 0 \\ 0 \end{pmatrix}$$

and the following nonzero matrix products in (2.2):

$$A_1B = A_1A_1B = \begin{pmatrix} 1 \\ 0 \\ 0 \end{pmatrix}, \; A_2B = A_2A_1B = \begin{pmatrix} 0 \\ 1 \\ 2 \end{pmatrix}, \; A_2A_2B = \begin{pmatrix} 5 \\ 8 \\ 16 \end{pmatrix}$$

that this system in not totally controllable.

Example 3.3: With the same method, we get the following four-dimensional classes of systems which are not totally controllable:

$$x' = \begin{pmatrix} * & * & * & * \\ * & * & * & * \\ * & * & * & * \\ 0 & 0 & 0 & * \end{pmatrix} x + \begin{pmatrix} * & 0 \\ 0 & * \\ 0 & 0 \\ 0 & 0 \end{pmatrix} \begin{pmatrix} u_1(t) \\ u_2(t) \end{pmatrix}$$

and

$$x' = \begin{pmatrix} * & * & * & * \\ * & * & * & * \\ 0 & 0 & * & * \\ 0 & 0 & * & * \end{pmatrix} x + \begin{pmatrix} * & 0 \\ 0 & * \\ 0 & 0 \\ 0 & 0 \end{pmatrix} \begin{pmatrix} u_1(t) \\ u_2(t) \end{pmatrix}.$$

ACKNOWLEDGMENT

We thank the referees for comments leading to the improvement of this note.

REFERENCES

[1] M. Fliess, "Some basic structural properties of generalized linear systems," *Syst. Control Lett.*, vol. 15, no. 5, pp. 391–396, 1990.

[2] E. B. Lee and L. Markus, *Foundations of Optimal Control Theory*, 2nd ed. Melbourne, Australia: Robert E. Krieger Publishing, 1986.

[3] H. Leiva and B. Lehman, "Algebraic Rank Test for Complete Controllability of Non-Autonomous Linear systems," Georgia Inst. Technol., Atlanta, GA, CDSNS 91–92, 1992.

[4] H. Leiva and H. Zambrano, "Rank condition for the controllability of a linear time-varying system," *Int. J. Control*, vol. 72, pp. 929–931, 1999.

[5] W. E. Schmitendorf and B. R. Barmish, "Null controllability of linear systems with constrained controls," *SIAM J. Control Optim.*, vol. 18, no. 4, pp. 327–345, 1980.

[6] L. M. Silverman and H. E. Meadows, "Controllability and observability in time-variable linear systems," *SIAM J. Control*, vol. 5, pp. 64–73, 1967.

[7] F. Szigeti, "A differential-algebraic condition for controllability and observability of time varying linear systems," *IEEE Proc. 31st Conf. Decision Control*, pp. 3088–3090, 1992.

[8] J. Wei and E. Norman, "On global representation of the solutions of linear differential equations as a product of exponentials," in *Proc. Amer. Math. Soc.*, vol. 15, 1964, pp. 327–334.

Range Identification for Perspective Vision Systems

W. E. Dixon, Y. Fang, D. M. Dawson, and T. J. Flynn

***Abstract*—In this note, a new observer is developed to determine range information (and, hence, the three-dimensional (3-D) coordinates) of an object feature moving with affine motion dynamics (or the more general Ricatti motion dynamics) with known motion parameters. The unmeasurable range information is determined from a single camera provided an observability condition is satisfied that has physical significance. To develop the observer, the perspective system is expressed in terms of the nonlinear feature dynamics. The structure of the proposed observer is inspired by recent disturbance observer results. The proposed technique facilitates a Lyapunov-based analysis that is less complex than the sliding-mode based analysis derived for recent observer designs. The analysis demonstrates that the 3-D task-space coordinates of the feature point can be asymptotically identified. Simulation results are provided that illustrate the performance of the observer in the presence of noise.**

***Index Terms*—Affine system, nonlinear observer, visual servoing.**

I. INTRODUCTION

The objective of most vision problems involves interpreting the motion of features of a three-dimensional (3-D) object through two-dimensional images that are projected perspectively[1] from the 3-D feature; hence, as stated in [6] vision systems are inherently perspective. Most research related to perspective systems have targeted the identification of the motion parameters (e.g., feature velocities) by using measureable state information. For example, for the following second-order system [6]:

$$\begin{bmatrix} \dot{x}_1 \\ \dot{x}_2 \end{bmatrix} = \begin{bmatrix} a_1 & a_2 \\ a_3 & a_4 \end{bmatrix} \begin{bmatrix} x_1 \\ x_2 \end{bmatrix} \tag{1}$$

the typical problem is to utilize the measureable states $x_1(t)$ and $x_2(t)$ to determine the unmeasurable parameters $a_i(t)\ \forall i = 1, 2, 3, 4$ and possibly the unknown initial conditions $x_1(t_0)$ and $x_2(t_0)$. An excellent overview of research that has targeted this and similar problems (typically using an extended Kalman filter) is provided in [5], [6], and [8].

In contrast to the class of perspective problems associated with using the measureable states to determine the parameters, several researchers have recently investigated the problem when the motion parameters are

Manuscript received February 12, 2003; revised May 8, 2003. Recommended by Associate Editor F. M. Callier. This work was supported in part by the Department of Energy Office of Biological and Environmental Research (OBER) Environmental Management Sciences Program (EMSP) project ID 82797 at ORNL, a subcontract to ORNL by the Florida Department of Citrus, by the National Science Foundation under Grant DMI-9457967, by the Office of Naval Research under Grant N00014-99-1-0589, a DOC Grant, and an ARO Automotive Center Grant.

W. E. Dixon is with the Engineering Science and Technology Division—Robotics, Oak Ridge National Laboratories, Oak Ridge, TN 37831-6305 USA (e-mail: dixonwe@ornl.gov).

Y. Fang is with the Department of Automation and Computer-Aided Engineering, The Chinese University of Hong Kong, Shatin, N. T. Hong Kong.

D. M. Dawson is with the Department of Electrical And Computer Engineering, Clemson University, Clemson, SC 29631-0915 USA.

T. J. Flynn is with the Science Applications International Corporation, Imagery Technology and Systems Division, Technology Research Group, Tucson, AZ 85711 USA.

Digital Object Identifier 10.1109/TAC.2003.820151

[1]Other projective models (e.g., orthographic projection) have also been used in literature for vision research; however, the most commonly accepted model is the perspective projection.

known along with the image-space feature coordinates, and the goal is to determine the unknown states (i.e., the actual 3-D position of the feature). For example, a recursive identifier based observer was developed in [8] to exponentially identify range information of features (i.e., points, lines, and planar curves) on an affine plane from successive images of a camera that is moving in a known manner (i.e., with known motion parameters). In [1], Chen and Kano develop a new observer for a more general perspective system that exponentially forces the observation error to an arbitrarily small neighborhood [i.e., uniformly ultimately bounded (UUB)].

In this note, we develop an observer to determine range information (and, hence, the 3-D task-space coordinates) for an object feature moving with general affine motion dynamics with known motion parameters. As in [1] and [11], the perspective system examined in this note and the preliminary work in [3] is more general than the skew-symmetric system examined in [8]. The unmeasurable range information is determined from a single camera provided an observability condition similar to [1] and [8] is satisfied. As stated in [6], many geometric structures of a perspective system are lost if they are studied via linearization; hence, to develop the observer, the perspective system is transformed into a nonlinear dynamic system (i.e., the image-space feature dynamics). Based on the nonlinear dynamics of the image-space signals an observer is designed that is inspired by the recent disturbance observer results in [4] and [9]. The structure of the proposed observer facilitates a Lyapunov-based analysis that is less complex than the sliding-mode based analysis derived for the observer design of [1]. More significantly, the unknown states can be exactly determined rather than "almost" determined as in the UUB result in [1]. The analysis demonstrates that the 3-D task-space coordinates of the feature point can be asymptotically identified. The proposed observer can also be applied to object motion described by Riccati dynamics and can be extended to n-dimensional perspective systems. Simulation results are provided that illustrate the performance of the observer.

The note is organized in the following manner. In Section II, the general perspective system is presented and the image-space feature dynamics are determined. In Section III, the observation problem is defined, and the observer is developed. The observation error is proven to be asymptotically regulated through a Lyapunov-based analysis in Section IV. Simulation results are provided in Section V, and concluding remarks are made in Section VI.

II. Perspective System

Consider an object feature undergoing an affine motion as follows [1], [11]:

$$\begin{bmatrix} \dot{x}_1 \\ \dot{x}_2 \\ \dot{x}_3 \end{bmatrix} = \begin{bmatrix} a_{11} & a_{12} & a_{13} \\ a_{21} & a_{22} & a_{23} \\ a_{31} & a_{32} & a_{33} \end{bmatrix} \begin{bmatrix} x_1 \\ x_2 \\ x_3 \end{bmatrix} + \begin{bmatrix} b_1 \\ b_2 \\ b_3 \end{bmatrix} \tag{2}$$

where $x_1(t)$, $x_2(t)$, $x_3(t) \in \mathbb{R}$ denote the unmeasurable task-space coordinates of an object feature along the X, Y, and Z axes of an inertial reference frame, respectively, with the Z axis being perpendicular with an image plane formed by a camera (i.e., the coordinate $x_3(t)$ denotes the depth from the image plane to the task-space object feature along the optical axis Z). In (2), the parameters $a_{i,j}(t) \in \mathbb{R}$ and $b_i(t)$ $\forall i, j = 1, 2, 3$ denote the known motion parameters [1], [11]. The affine motion dynamics introduced in (2) are expressed in a general form that describes an object motion that undergoes a rotation, translation, and linear deformation [11]. The measurable image-space coordinate of a feature, denoted by $y(t) \in \mathbb{R}^2$, is given as follows:

$$y \triangleq \begin{bmatrix} y_1 & y_2 \end{bmatrix}^T = \begin{bmatrix} \frac{x_1}{x_3} & \frac{x_2}{x_3} \end{bmatrix}^T. \tag{3}$$

The affine dynamics introduced in (2) and the image-space signal introduced in (3) define the perspective system [1]. After taking the time derivative of (3) and utilizing (2), the image-space trajectory of the object feature can be obtained as follows:

$$\dot{y}_1 = \frac{a_{11}x_1 + a_{12}x_2 + a_{13}x_3 + b_1}{x_3} - \frac{x_1\left(a_{31}x_1 + a_{32}x_2 + a_{33}x_3 + b_3\right)}{x_3^2}. \tag{4}$$

$$\dot{y}_2 = \frac{a_{21}x_1 + a_{22}x_2 + a_{23}x_3 + b_2}{x_3} - \frac{x_2\left(a_{31}x_1 + a_{32}x_2 + a_{33}x_3 + b_3\right)}{x_3^2}. \tag{5}$$

To facilitate subsequent analysis, the time derivative of the inverse of $x_3(t)$ is determined as follows:

$$\frac{d}{dt}\left(\frac{1}{x_3}\right) = \frac{-a_{31}x_1 - a_{32}x_2 - a_{33}x_3 - b_3}{x_3^2}. \tag{6}$$

By utilizing (3), the expressions given in (4)–(6) can be rewritten as follows:

$$\dot{y}_1 = a_{13} + (a_{11} - a_{33})\, y_1 + a_{12}y_2 - a_{31}y_1^2 - a_{32}y_1y_2 + f_1 \tag{7}$$

$$\dot{y}_2 = a_{23} + a_{21}y_1 + (a_{22} - a_{33})\, y_2 - a_{32}y_2^2 - a_{31}y_1y_2 + f_2 \tag{8}$$

$$\frac{d}{dt}\left(\frac{1}{x_3}\right) = -\frac{1}{x_3}\left(a_{31}y_1 + a_{32}y_2 + a_{33}\right) - \frac{b_3}{x_3^2} \tag{9}$$

where $f_1(x_3, y_1)$, $f_2(x_3, y_2) \in \mathbb{R}$ are unmeasurable signals[2] defined as follows:

$$f_1 \triangleq \frac{1}{x_3}\left(b_1 - b_3y_1\right) \tag{10}$$

$$f_2 \triangleq \frac{1}{x_3}\left(b_2 - b_3y_2\right). \tag{11}$$

For the perspective system given in (2) and (3), the following assumptions are made [1].

Assumption 1: The known motion parameters $a_{i,j}(t)$ and $b_i(t)$ $\forall i, j = 1, 2, 3$ introduced in (2) are bounded functions of time, the parameters $a_{i,j}(t)$ are first order differentiable, and the parameters $b_i(t)$ are second-order differentiable.

Assumption 2: The image-space feature coordinates $y_1(t)$ and $y_2(t)$ are bounded functions of time (i.e., $y_1(t), y_2(t) \in \mathcal{L}_\infty$).

Assumption 3: The object feature motion avoids the degenerate case where the feature intersects the image plane. That is, $x_3(t) > \varepsilon_0$ where $\varepsilon_0 \in \mathbb{R}$ is an arbitrarily small positive constant and, hence, $1/x_3(t) \in \mathcal{L}_\infty$. Moreover, we also assume that $x_3(t) \in \mathcal{L}_\infty$.

Remark 1: Assumptions 2 and 3 are standard assumptions (see also [1] and [8]) that are practically properties of the physical system rather than assumptions.

Remark 2: Based on Assumptions 1–3, the expressions given in (2) and (7)–(11) can be used to determine that $\dot{x}_3(t)$, $\dot{y}(t)$, $d/dt\,(1/x_3(t))$, $f_1(x_3, y_1)$, $f_2(x_3, y_2) \in \mathcal{L}_\infty$. Given that these signals are bounded, the development provided in the Appendix can be used along with Assumptions 1–3 to also determine that $\dot{f}_1(\cdot)$, $\dot{f}_2(\cdot)$, $\ddot{f}_1(\cdot)$, and $\ddot{f}_2(\cdot) \in \mathcal{L}_\infty$.

III. Observation Problem

A. Objective

The objective in this note is to determine the unmeasurable state $x_3(t)$ of the perspective vision system described by (2) and (3). From (3) and the fact that $y_1(t)$ and $y_2(t)$ are measurable, it is clear that if $x_3(t)$ is identified then the complete 3-D task-space coordinate of

[2]The signals $f_1(x_3, y_1)$, and $f_2(x_3, y_2)$ are unmeasurable due to a dependence on the unmeasurable state $x_3(t)$.

the feature can be determined. To achieve this objective, an observer is constructed based on the unmeasurable image-space dynamics for $y(t)$. To quantify the performance of the observer, a measurable observer estimation error signal, denoted by $e(t) \in \mathbb{R}^2$, is defined as follows:

$$e \triangleq [\, e_1 \quad e_2 \,]^T = [\, y_1 - \hat{y}_1 \quad y_2 - \hat{y}_2 \,]^T \tag{12}$$

where $\hat{y}(t) \triangleq [\hat{y}_1(t), \hat{y}_2(t)]^T \in \mathbb{R}^2$ denotes a subsequently designed observer signal. To facilitate the subsequent development, a filtered observation error signal, denoted by $r(t) \in \mathbb{R}^2$, is designed as follows:

$$r \triangleq [\, r_1 \quad r_2 \,]^T = [\, \dot{e}_1 + \alpha_1 e_1 \quad \dot{e}_2 + \alpha_2 e_2 \,]^T \tag{13}$$

where α_1, $\alpha_2 \in \mathbb{R}$ denote positive constant gains. Based on the dynamics in (7) and (8) and the definitions introduced in (12) and (13), it is clear that $r(t)$ is unmeasurable due to the fact that $\dot{y}(t)$ is a function of the unmeasurable disturbance terms $f_1(x_3, y_1)$ and $f_2(x_3, y_2)$. The subsequent development will target the design of estimates for $f_1(x_3, y_1)$ and $f_2(x_3, y_2)$ based on the strategy that if the mismatch between the estimates and the disturbance terms $f_1(x_3, y_1)$ and $f_2(x_3, y_2)$ can be driven to zero, then $x_3(t)$ can be identified by exploiting the fact that $b_i(t)\ \forall i = 1, 2, 3$ and the states $y_1(t)$ and $y_2(t)$ are measurable. Specifically, from (10) and (11), the inverse of the square of $x_3(t)$ can be determined as follows:

$$\left(\frac{1}{x_3}\right)^2 = \frac{f_1^2 + f_2^2}{(b_1 - b_3 y_1)^2 + (b_2 - b_3 y_2)^2}\,. \tag{14}$$

Based on the structure of (14), it is clear that the following observability condition must be satisfied:

$$(b_1 - b_3 y_1)^2 + (b_2 - b_3 y_2)^2 > 0\,. \tag{15}$$

That is, $x_3(t)$ can be identified once the mismatch between the disturbance terms $f_1(x_3, y_1)$ and $f_2(x_3, y_2)$ and the respective estimates are driven to zero.

Remark 3: The observability condition introduced in (15) is not required by the subsequent analysis to prove that the observer design remains bounded. That is, the subsequent analysis can be used to prove that $f_1(x_3, y_1)$ and $f_2(x_3, y_2)$ can be identified independently of (15); however, (15) is required to prove that $x_3(t)$ can be identified. In [8], a discussion is provided regarding the physical justification of (15) with regard to the focus of expansion.

B. Observer Design and Error System

By taking the time-derivative of (12) the following error dynamics can be obtained for $e(t)$:

$$\dot{e} = \dot{y} - \dot{\hat{y}}\,. \tag{16}$$

Based on the structure of (7), (8), and (16), the elements of the observer signal $\hat{y}(t)$ are designed as follows:

$$\dot{\hat{y}}_1 = a_{13} + (a_{11} - a_{33})\, y_1 + a_{12} y_2 - a_{31} y_1^2 - a_{32} y_1 y_2 + \hat{f}_1 \tag{17}$$

$$\dot{\hat{y}}_2 = a_{23} + a_{21} y_1 + (a_{22} - a_{33})\, y_2 - a_{32} y_2^2 - a_{31} y_1 y_2 + \hat{f}_2 \tag{18}$$

where $\hat{f}_1(t)$, $\hat{f}_2(t) \in \mathbb{R}$ denote subsequently designed estimates for the unmeasurable signals $f_1(t)$ and $f_2(t)$ introduced in (7) and (8). After substituting (7), (8), (17), and (18) into (16), the following error dynamics are obtained:

$$\dot{e} = [\, f_1 - \hat{f}_1 \quad f_2 - \hat{f}_2 \,]^T\,. \tag{19}$$

By taking the time-derivative of (13), the following error dynamics can be obtained for $r(t)$:

$$\dot{r} = \begin{bmatrix} \dot{f}_1 - \dot{\hat{f}}_1 + \alpha_1 \left(f_1 - \hat{f}_1\right) \\ \dot{f}_2 - \dot{\hat{f}}_2 + \alpha_2 \left(f_2 - \hat{f}_2\right) \end{bmatrix} \tag{20}$$

where (19) and the time derivative of (19) have been utilized. Based on the structure of (20) and the subsequent analysis, the estimates $\hat{f}_1(t)$ and $\hat{f}_2(t)$ are designed as follows[3]:

$$\dot{\hat{f}}_1 = -(k_{s1} + \alpha_1)\hat{f}_1 + \gamma_1 \mathrm{sgn}(e_1) + \alpha_1 k_{s1} e_1 \tag{21}$$

$$\dot{\hat{f}}_2 = -(k_{s2} + \alpha_2)\hat{f}_2 + \gamma_2 \mathrm{sgn}(e_2) + \alpha_2 k_{s2} e_2 \tag{22}$$

where k_{s1}, k_{s2}, γ_1, $\gamma_2 \in \mathbb{R}$ denote constant observer gains and the notation $\mathrm{sgn}(\cdot)$ is used to indicate the standard, signum function. After substituting (21) and (22) into (20), and then adding and subtracting the terms $k_{s1} f_1(x_3, y_1)$ and $k_{s2} f_2(x_3, y_2)$, the following expression can be obtained:

$$\dot{r} = \eta - \begin{bmatrix} k_{s1} r_1 + \gamma_1 \mathrm{sgn}(e_1) \\ k_{s2} r_2 + \gamma_2 \mathrm{sgn}(e_2) \end{bmatrix} \tag{23}$$

where $\eta(t) \triangleq [\, \eta_1 \quad \eta_2 \,]^T \in \mathbb{R}^2$ is defined as follows:

$$\eta \triangleq \begin{bmatrix} \dot{f}_1 + (k_{s1} + \alpha_1)\, f_1 \\ \dot{f}_2 + (k_{s2} + \alpha_2)\, f_2 \end{bmatrix}. \tag{24}$$

Remark 4: The time derivative of (24) can be determined as follows:

$$\dot{\eta} = \begin{bmatrix} \ddot{f}_1 + (k_{s1} + \alpha_1)\, \dot{f}_1 \\ \ddot{f}_2 + (k_{s2} + \alpha_2)\, \dot{f}_2 \end{bmatrix}. \tag{25}$$

From (24) and (25), the statements in Remark 2 can be used to conclude that $\eta(t), \dot{\eta}(t) \in \mathcal{L}_\infty$.

Remark 5: The structure of the disturbance observer given by (21) and (22) contains discontinuous terms; however, it is interesting to note that the overall structure of the observer yields the continuous signals $\hat{f}_1(t)$ and $\hat{f}_2(t)$. That is, after a close examination of (17) and (18), it is clear that $\dot{\hat{y}}_1(t)$ and $\dot{\hat{y}}_2(t)$ only contain the low pass filtered outputs $\hat{f}_1(t)$ and $\hat{f}_2(t)$ of the discontinuous terms in (21) and (22).

IV. Analysis

The following theorem and associated proof can be used to conclude that the observer design of (17), (18), (21), and (22) can be used to identify the unmeasurable state $x_3(t)$.

Theorem 1: Given the perspective system in (2) and (3), the unmeasurable state $x_3(t)$ (and, hence, the 3-D task-space coordinates of the object feature) can be asymptotically determined using the observer design given in (17), (18), (21), and (22) provided the constants γ_1 and γ_2 introduced in (21) and (22) are selected according to the following sufficient conditions:

$$\gamma_1 \geq |\eta_1| + |\dot{\eta}_1| \qquad \gamma_2 \geq |\eta_2| + |\dot{\eta}_2| \tag{26}$$

where $\eta(t)$ is defined in (24), and the observability condition introduced in (15) is satisfied.

Proof: To prove Theorem 1, we first define a nonnegative function $V(t)$ as follows:

$$V \triangleq \frac{1}{2} r^{\Upsilon} r\,. \tag{27}$$

[3]The design of the estimates $\hat{\boldsymbol{f}}_1(\boldsymbol{t})$ and $\hat{\boldsymbol{f}}_2(\boldsymbol{t})$ is inspired by the development given in [4] and [9].

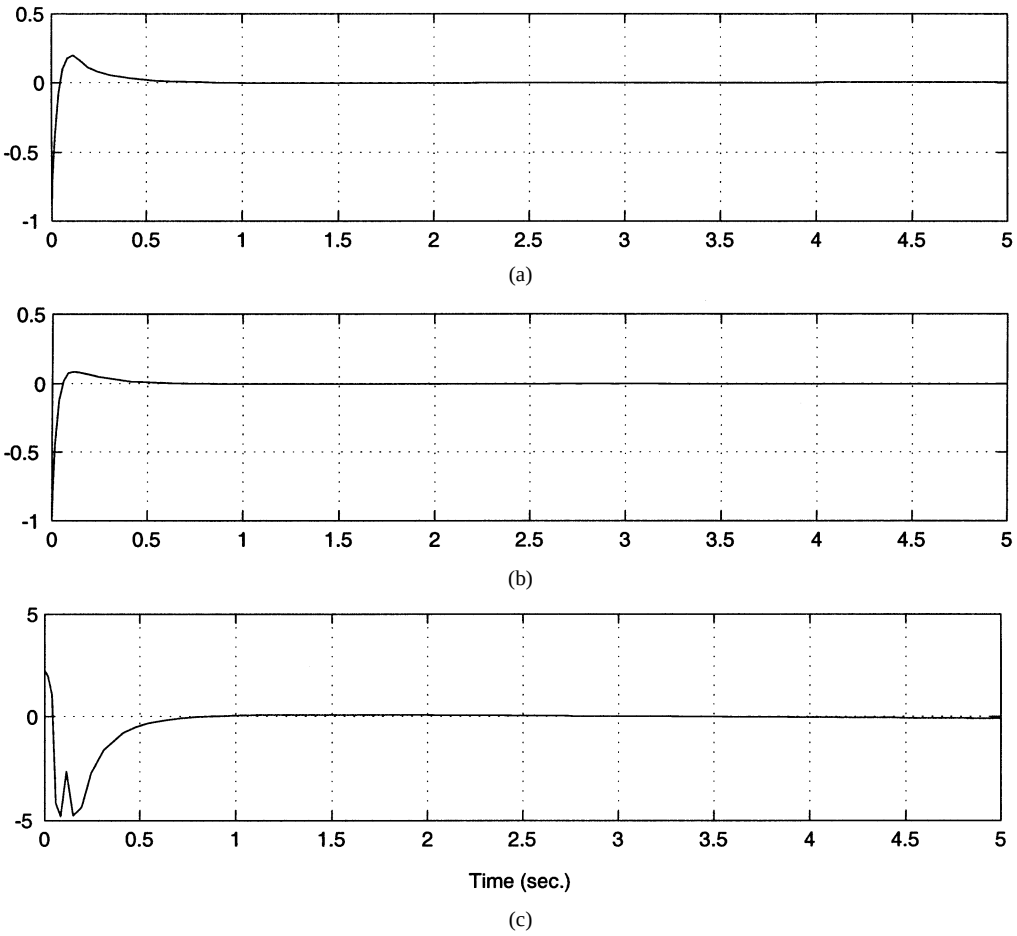

Fig. 1. Observation mismatch between (a) $\boldsymbol{f}_1(\boldsymbol{t})$ and $\hat{\boldsymbol{f}}_1(\boldsymbol{t})$, (b) $\boldsymbol{f}_2(\boldsymbol{t})$ and $\hat{\boldsymbol{f}}_2(\boldsymbol{t})$, and (c) $\boldsymbol{x}_3(\boldsymbol{t})$ and the estimated value from (14) with no measurement noise.

After taking the time derivative of (27) and substituting for the error system dynamics given in (23), the following expression can be obtained:

$$\dot{V} = -k_{s1}r_1^2 - k_{s2}r_2^2 + (\dot{e}_1 + \alpha_1 e_1)(\eta_1 - \gamma_1 \mathrm{sgn}(e_1)) + (\dot{e}_2 + \alpha_2 e_2)(\eta_2 - \gamma_2 \mathrm{sgn}(e_2)). \quad (28)$$

After integrating (28) and exploiting the fact that

$$\xi \cdot \mathrm{sgn}(\xi) = |\xi|$$

the following inequality can be obtained:

$$V(t) \le V(t_0) - \int_{t_0}^{t} \left(k_{s1}r_1^2(\sigma) + k_{s2}r_2^2(\sigma)\right) d\sigma + \alpha_1 \int_{t_0}^{t} |e_1(\sigma)| \left(|\eta_1(\sigma)| - \gamma_1\right) d\sigma + \Omega_1 + \alpha_2 \int_{t_0}^{t} |e_2(\sigma)| \left(|\eta_2(\sigma)| - \gamma_2\right) d\sigma + \Omega_2 \quad (29)$$

where the auxiliary terms $\Omega_1(t), \Omega_2(t) \in \mathbb{R}$ are defined as follows:

$$\Omega_1 \triangleq \int_{t_0}^{t} \dot{e}_1(\sigma)\eta_1(\sigma)\, d\sigma - \gamma_1 \int_{t_0}^{t} \dot{e}_1(\sigma)\mathrm{sgn}(e_1(\sigma)) d\sigma \quad (30)$$

$$\Omega_2 \triangleq \int_{t_0}^{t} \dot{e}_2(\sigma)\eta_2(\sigma)\, d\sigma - \gamma_2 \int_{t_0}^{t} \dot{e}_2(\sigma)\mathrm{sgn}(e_2(\sigma)) d\sigma. \quad (31)$$

After evaluating the integral expressions in (30), the following expressions can be obtained:

$$\begin{aligned}\Omega_1 =& e_1(\sigma)\eta_1(\sigma)|_{t_0}^{t} d\sigma - \int_{t_0}^{t} e_1(\sigma)\dot{\eta}_1(\sigma)\, d\sigma - \gamma_1 |e_1(\sigma)|\,|_{to}^{t} \\ =& e_1(t)\eta_1(t) - \int_{t_0}^{t} e_1(\sigma)\dot{\eta}_1(\sigma)\, d\sigma - \gamma_1 |e_1(t)| \\ & - e_1(t_0)\eta_1(t_0) + \gamma_1 |e_1(t_0)|. \end{aligned} \quad (32)$$

By performing the same operations, $\Omega_2(t)$ can be evaluated as follows:

$$\Omega_2 = e_2(t)\eta_2(t) - \int_{t_0}^{t} e_2(\sigma)\dot{\eta}_2(\sigma)\, d\sigma - \gamma_2 |e_2(t)| - e_2(t_0)\eta_2(t_0) + \gamma_2 |e_2(t_0)|. \quad (33)$$

After substituting (32) and (33) into (29) and performing some algebraic manipulation, the following inequality can be obtained:

$$V(t) \le V(t_0) - \int_{t_0}^{t} \left(k_{s1}r_1^2(\sigma) + k_{s2}r_2^2(\sigma)\right) d\sigma + \Omega_3 + \zeta_0 \quad (34)$$

where the auxiliary terms $\Omega_3(t), \zeta_0 \in \mathbb{R}$ are defined as follows:

$$\begin{aligned}\Omega_3 \triangleq& \alpha_1 \int_{t_0}^{t} |e_1(\sigma)| \left(|\eta_1(\sigma)| + |\dot{\eta}_1(\sigma)| - \gamma_1\right) d\sigma \quad (35) \\ & + \alpha_2 \int_{t_0}^{t} |e_2(\sigma)| \left(|\eta_2(\sigma)| + |\dot{\eta}_2(\sigma)| - \gamma_2\right) d\sigma \\ & + |e_1(t)| \left(|\eta_1(t)| - \gamma_1\right) + |e_2(t)| \left(|\eta_2(t)| - \gamma_2\right) \\ \zeta_0 \triangleq& -e_1(t_0)\eta_1(t_0) + \gamma_1 |e_1(t_0)| \\ & - e_2(t_0)\eta_2(t_0) + \gamma_2 |e_2(t_0)|. \end{aligned} \quad (36)$$

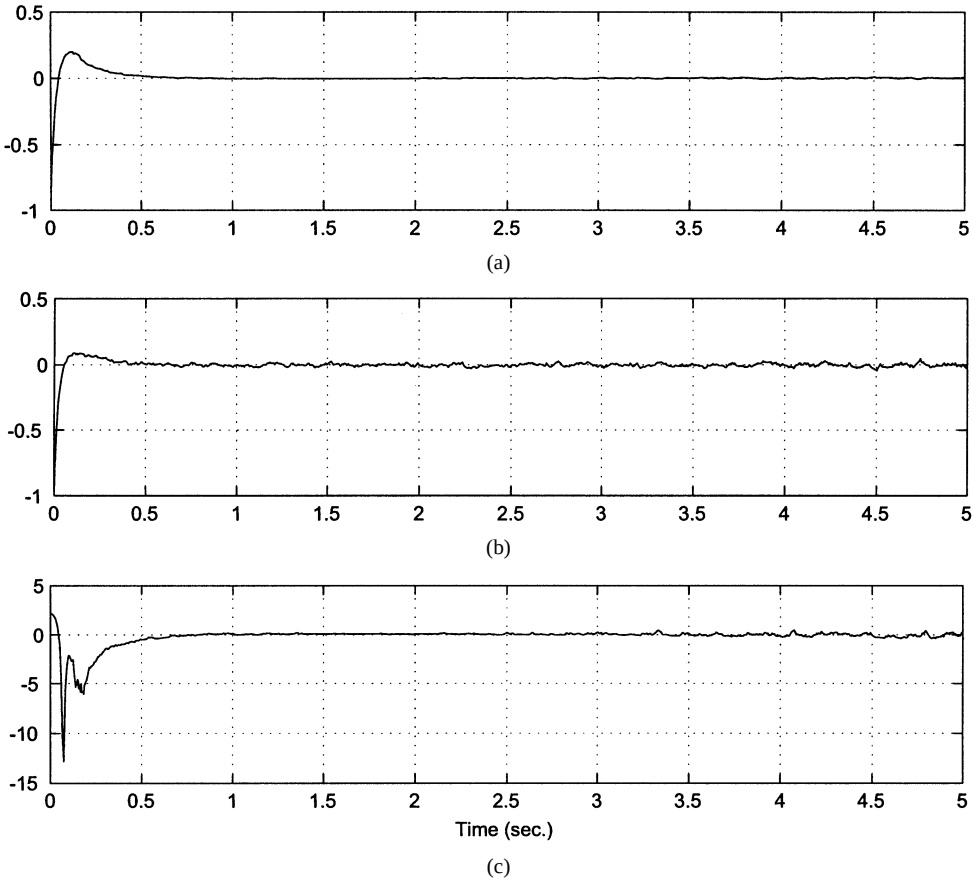

Fig. 2. Observation mismatch between (a) $\boldsymbol{f_1(t)}$ and $\hat{\boldsymbol{f}}_1(\boldsymbol{t})$, (b) $\boldsymbol{f_2(t)}$ and $\hat{\boldsymbol{f}}_2(\boldsymbol{t})$, and (c) $\boldsymbol{x_3(t)}$ and the estimated value from (14) with 1% measurement noise.

Provided the constants γ_1 and γ_2 are selected according to the inequalities introduced in (26), $\Omega_3(t)$ will always be negative or zero; hence, the following upper bound can be developed:

$$V(t) \leq V(t_0) - \int_{t_0}^{t} \left(k_{s1} r_1^2(\sigma) + k_{s2} r_2^2(\sigma)\right) d\sigma + \zeta_0. \tag{37}$$

From (27) and (37), the following inequalities can be determined:

$$V(t_0) + \zeta_0 \geq V(t) \geq 0 \tag{38}$$

hence, $r(t) \in \mathcal{L}_\infty$. The expression in (37) can be used to determine that

$$\int_0^\infty \left(k_{s1} r_1^2(\sigma) + k_{s2} r_2^2(\sigma)\right) d\sigma \leq V(0) + \zeta_0 - V(\infty) \leq V(0) + \zeta_0 < \infty. \tag{39}$$

By definition, (39) can now be used to prove that $r(t) \in \mathcal{L}_2$. From the fact that $r(t) \in \mathcal{L}_\infty$, (12) and (13) can be used to prove that $e(t)$, $\dot{e}(t)$, $\hat{y}(t)$, and $\dot{\hat{y}}(t) \in \mathcal{L}_\infty$. The expressions in (17), (18), (21), and (22) can be used to determine that $\hat{f}_1(t)$, $\hat{f}_2(t)$, $\dot{\hat{f}}_1(t)$, and $\dot{\hat{f}}_2(t) \in \mathcal{L}_\infty$. Based on the facts that $f_1(x_3, y_1)$, $f_2(x_3, y_2)$, $\dot{f}_1(\cdot)$, and $\dot{f}_2(\cdot) \in \mathcal{L}_\infty$, the expressions in (23) and (24) can be used to prove that $\eta(t), \dot{r}(t) \in \mathcal{L}_\infty$. Based on the fact that $r(t), \dot{r}(t) \in \mathcal{L}_\infty$ and that $r(t) \in \mathcal{L}_2$, Barbalat's Lemma [10] can be used to prove that $\|r(t)\| \to 0$ as $t \to \infty$; hence, [2, Lemma 1.6] can be used to prove that $\|e(t)\| \to 0$ and $\|\dot{e}(t)\| \to 0$ as $t \to \infty$. Based on the fact that $\|e(t)\| \to 0$ and $\|\dot{e}(t)\| \to 0$ as $t \to \infty$, the expression given in (12) can be used to determine that $\hat{y}_1(t)$ and $\hat{y}_2(t)$ approach $y_1(t)$ and $y_2(t)$ as $t \to \infty$, respectively. Therefore, the expression in (19) can be used to determine that $\hat{f}_1(t)$ and $\hat{f}_2(t)$ approach $f_1(t)$ and $f_2(t)$ as $t \to \infty$. If the observability condition given in (15) is satisfied (i.e., if either $f_1(x_3, y_1)$ or $f_2(x_3, y_2)$ are nonzero), then the result that $\hat{f}_1(t)$ and $\hat{f}_2(t)$ approach $f_1(t)$ and $f_2(t)$ as $t \to \infty$, the fact that the parameters $b_i(t)\, \forall i = 1, 2, 3$ are assumed to be known, and the fact that the image-space signal $y(t)$ is measurable can be used to identify the unknown task-space parameter $x_3(t)$ from (14). Once $x_3(t)$ is identified, the complete 3-D task-space coordinates of the object feature can be determined from (3). □

Remark 2: In addition to the general affine motion model considered in (2), several results in literature have examined the following Riccati motion dynamics (e.g., [1], [5], and [7])

$$\begin{bmatrix} \dot{x}_1 \\ \dot{x}_2 \\ \dot{x}_3 \end{bmatrix} = \begin{bmatrix} a_{11} & a_{12} & a_{13} \\ a_{21} & a_{22} & a_{23} \\ a_{31} & a_{32} & a_{33} \end{bmatrix} \begin{bmatrix} x_1 \\ x_2 \\ x_3 \end{bmatrix} + \begin{bmatrix} b_1 \\ b_2 \\ b_3 \end{bmatrix} + \begin{bmatrix} c_1 & c_2 & c_3 & 0 & 0 & 0 \\ 0 & c_1 & 0 & c_2 & c_3 & 0 \\ 0 & 0 & c_1 & 0 & c_2 & c_3 \end{bmatrix} \begin{bmatrix} x_1^2 \\ x_1 x_2 \\ x_1 x_3 \\ x_2^2 \\ x_2 x_3 \\ x_3^2 \end{bmatrix}. \tag{40}$$

For these dynamics, the same expressions given in (7)–(11) can be obtained and, hence, the observer design in (17), (18), (21), and (22) still applies for this motion field. Note that the observer developed in [1] for the affine motion dynamics in (2) can also be applied to the motion dynamics in (40). As in [1], the observer system design in this note can also be extended to general n-dimensional perspective systems.

V. Simulation Examples

In this section, numerical simulation results are presented to demonstrate the performance of the algorithm developed in (17)–(22). In the first example, the image-space data is considered to be noise free, and in the second example, the measured image data is assumed to be corrupted by 1% with random noise as in [1].

Example 1: For this example, the movement of an object in the task-space is described by the following perspective system [1]:

$$\begin{bmatrix} \dot{x}_1 \\ \dot{x}_2 \\ \dot{x}_3 \end{bmatrix} = \begin{bmatrix} -0.2 & 0.4 & -0.6 \\ 0.1 & -0.2 & 0.3 \\ 0.3 & -0.4 & 0.4 \end{bmatrix} \begin{bmatrix} x_1 \\ x_2 \\ x_3 \end{bmatrix} + \begin{bmatrix} 0.5 \\ 0.25 \\ 0.3 \end{bmatrix} \tag{41}$$

where

$$[\, x_1(0) \quad x_2(0) \quad x_3(0)\,]^T = [\, 1 \quad 1.5 \quad 2.5\,]^T. \tag{42}$$

The initial conditions for $\hat{y}_1(t)$, $\hat{y}_2(t)$, $\hat{f}_1(t)$, and $\hat{f}_2(t)$ are given as follows:

$$\begin{array}{cc} \hat{y}_1(0) = y_1(0) & \hat{y}_2(0) = y_2(0) \\ \hat{f}_1(0) = 1 & \hat{f}_2(0) = 1. \end{array} \tag{43}$$

The observer gains were selected as follows:

$$\begin{aligned} k_{s1} &= 30 \quad \alpha_1 = 5 \quad \gamma_1 = 1 \\ k_{s2} &= 40 \quad \alpha_2 = 5 \quad \gamma_2 = 0.1. \end{aligned} \tag{44}$$

After implementing the observer with the gains selected as in (44), the resulting observation mismatch between $f_1(t)$ and $\hat{f}_1(t)$ and $f_2(t)$ and $\hat{f}_2(t)$ is depicted in Fig. 1 along with the mismatch between $x_3(t)$ and the estimated value from (14).

Example 2: For this example, the same system from Example 1 was simulated with 1% random noise injected on the measured image-space signals $y_1(t)$ and $y_2(t)$. Using the same gain selections as in (44), the resulting observer mismatch is depicted in Fig. 2. Fig. 2 also illustrates the mismatch between $x_3(t)$ and the estimated value.

The results depicted in Figs. 1 and 2 indicate that the developed observer strategy can be used to identify the range parameter using a single camera provided the observability condition is satisfied. In comparison with the simulation results for the observer presented in [1], the results in Figs. 1 and 2 illustrate that the developed observer has at least similar transient performance (although the steady-state response of the observer in [1] is only proven to be bounded to a region about the origin). In comparison with the simulation results for the observer presented in [8], the results in Figs. 1 and 2 illustrate superior transient response. The impact of these results are that the developed observer can be used to enable a monocular vision system to identify the range parameter (even in the presence of sensor noise) of an object moving (with known motion parameters) with an affine or Riccati motion dynamics.

VI. Conclusion

In this note, a new observer inspired by the development in [9] was developed to identify an unmeasurable range signal (and, hence, the 3-D task-space coordinates of an object feature) via a single camera given the motion parameters of a general affine system (or Riccati system). To develop the observer the affine perspective system is transformed into the nonlinear feature dynamics. Through a Lyapunov-based analysis, the observer was proven to asymptotically regulate the observation errors. Simulation results are provided that illustrate the performance of the observer even in the presence of image noise.

Appendix

To prove that $\dot{f}_1(\cdot)$, $\dot{f}_2(\cdot) \in \mathcal{L}_\infty$, the time derivative of (10) and (11) is determined as follows:

$$\dot{f}_1 = \frac{1}{x_3}\left(\dot{b}_1 - \dot{b}_3 y_1 - b_3 \dot{y}_1\right) + \frac{d}{dt}\left(\frac{1}{x_3}\right)(b_1 - b_3 y_1) \tag{45}$$

$$\dot{f}_2 = \frac{1}{x_3}\left(\dot{b}_2 - \dot{b}_3 y_2 - b_3 \dot{y}_2\right) + \frac{d}{dt}\left(\frac{1}{x_3}\right)(b_2 - b_3 y_2). \tag{46}$$

The facts that $\dot{y}(t)$, $d/dt\,(1/x_3(t)) \in \mathcal{L}_\infty$ can be used along with Assumptions 1–3 to conclude from (45) and (46) that $\dot{f}_1(\cdot)$, and $\dot{f}_2(\cdot) \in \mathcal{L}_\infty$. To prove that $\ddot{f}_1(\cdot)$, $\ddot{f}_2(\cdot) \in \mathcal{L}_\infty$, the time derivative of (45) and (46) can be determined as follows:

$$\begin{aligned} \ddot{f}_1 =& \frac{d}{dt}\left(\frac{1}{x_3}\right)\left(\dot{b}_1 - \dot{b}_3 y_1 - b_3 \dot{y}_1\right) \\ &+ \frac{1}{x_3}\left(\ddot{b}_1 - \ddot{b}_3 y_1 - 2\dot{b}_3 \dot{y}_1 - b_3 \ddot{y}_1\right) \\ &+ \frac{d^2}{dt^2}\left(\frac{1}{x_3}\right)(b_1 - b_3 y_1) + \frac{d}{dt}\left(\frac{1}{x_3}\right)\left(\dot{b}_1 - \dot{b}_3 y_1 - b_3 \dot{y}_1\right) \end{aligned} \tag{47}$$

$$\begin{aligned} \ddot{f}_2 =& \frac{d}{dt}\left(\frac{1}{x_3}\right)\left(\dot{b}_2 - \dot{b}_3 y_2 - b_3 \dot{y}_2\right) \\ &+ \frac{1}{x_3}\left(\ddot{b}_2 - \ddot{b}_3 y_2 - 2\dot{b}_3 \dot{y}_2 - b_3 \ddot{y}_2\right) \\ &+ \frac{d^2}{dt^2}\left(\frac{1}{x_3}\right)(b_2 - b_3 y_2) + \frac{d}{dt}\left(\frac{1}{x_3}\right)\left(\dot{b}_2 - \dot{b}_3 y_2 - b_3 \dot{y}_2\right) \end{aligned} \tag{48}$$

where

$$\begin{aligned} \ddot{y}_1 =& \dot{a}_{13} + (\dot{a}_{11} - \dot{a}_{33})\, y_1 + (a_{11} - a_{33})\, \dot{y}_1 \\ &+ \dot{a}_{12} y_2 + a_{12} \dot{y}_2 - \dot{a}_{31} y_1^2 - 2 a_{31} y_1 \dot{y}_1 \\ &- \dot{a}_{32} y_1 y_2 - \dot{y}_1 y_2 - a_{32} y_1 \dot{y}_2 + \dot{f}_1 \end{aligned} \tag{49}$$

$$\begin{aligned} \ddot{y}_2 =& \dot{a}_{23} + \dot{a}_{21} y_1 + a_{21} \dot{y}_1 + (\dot{a}_{22} - \dot{a}_{33})\, y_2 \\ &+ (a_{22} - a_{33})\, \dot{y}_2 \\ &- \dot{a}_{32} y_2^2 - 2 a_{32} y_2 \dot{y}_2 - \dot{a}_{31} y_1 y_2 - a_{31} \dot{y}_1 y_2 \\ &- a_{31} y_1 \dot{y}_2 + \dot{f}_2 \end{aligned} \tag{50}$$

$$\begin{aligned} \frac{d^2}{dt^2}\left(\frac{1}{x_3}\right) =& -\frac{d}{dt}\left(\frac{1}{x_3}\right)(a_{31} y_1 + a_{32} y_2 + a_{33}) \\ &- \frac{\dot{b}_3}{x_3^2} + 2\frac{b_3 \dot{x}_3}{x_3^3} - \frac{1}{x_3}(\dot{a}_{31} y_1 + a_{31} \dot{y}_1 + \dot{a}_{32} y_2 \\ &+ a_{32} \dot{y}_2 + \dot{a}_{33}) \end{aligned} \tag{51}$$

and the expressions given in (7)–(11) were utilized. The expressions given in (47)–(51), Assumptions 1–3, and the facts that $\dot{x}_3(t)$, $\ddot{y}(t)$, $d/dt\,(1/x_3(t))$, $f_1(x_3, y_1)$, $f_2(x_3, y_2) \in \mathcal{L}_\infty$ can now be used to prove that $\ddot{f}_1(\cdot)$, and $\ddot{f}_2(\cdot) \in \mathcal{L}_\infty$.

References

[1] X. Chen and H. Kano, "A new state observer for perspective systems," *IEEE Trans. Automat. Contr.*, vol. 47, pp. 658–663, Apr. 2002.

[2] D. M. Dawson, J. Hu, and T. C. Burg, *Nonlinear Control of Electric Machinery*. New York: Marcel Dekker, 1998.

[3] W. E. Dixon, Y. Fang, D. M. Dawson, and T. J. Flynn, "Range identification for perspective vision systems," *Proc. 2003 IEEE Amer. Control Conf.*, pp. 3448–3453, June 2003.

[4] Y. Fang, D. M. Dawson, M. Feemster, and N. Jalili, "Active interaction force identification for atomic force microscope applications," *Proc. IEEE Conf. Decision Control*, pp. 3678–3683, 2002.

[5] B. K. Ghosh, H. Inaba, and S. Takahashi, "Identification of riccati dynamics under perspective and orthographic observations," *IEEE Trans. Automat. Contr.*, vol. 45, pp. 1267–1278, July 2000.
[6] B. K. Ghosh, M. Jankovic, and Y. T. Wu, "Perspective problems in system theory and its application to machine vision," *J. Math. Syst., Estima., Control*, vol. 4, no. 1, pp. 3–38, 1994.
[7] B. K. Ghosh and E. P. Loucks, "A perspective theory for motion and shape estimation in machine vision," *SIAM J. Control Optim.*, vol. 33, no. 5, pp. 1530–1559, 1995.
[8] M. Jankovic and B. J. Ghosh, "Visually guided ranging from observations of points, lines and curves via an identifier based nonlinear observer," *Syst. Control Lett.*, vol. 25, pp. 63–73, 1995.
[9] Z. Qu and J.-X. Xu, "Model-based learning controls and their comparisons using Lyapunov direct method," *Asian J. Control*, vol. 4, no. 1, pp. 99–110, 2002.
[10] J. J. Slotine and W. Li, *Applied Nonlinear Control*. Upper Saddle River, NJ: Prentice-Hall, 1991.
[11] R. Y. Tsai and T. S. Huang, "Estimating three-dimensional motion parameters of a rigid planar patch," *IEEE Trans. Acoust., Speech, Signal Processing*, vol. ASSP-29, pp. 1147–1152, June 1981.

Transient Response Control via Characteristic Ratio Assignment

Y. C. Kim, L. H. Keel, and S. P. Bhattacharyya

***Abstract*—This note develops an approach to directly control the transient response of linear time-invariant control systems. We begin by considering all-pole transfer functions of order n for which we introduce a set of parameters α_i, $i = 1, \ldots n$ called the *characteristic ratios*. We also introduce a *generalized time constant* τ. We prove that α_1 and τ can be used to characterize the system overshoot to a step input and the speed of response, respectively. By independently adjusting α_1 and τ in all-pole systems, arbitrarily small or no overshoot as well as arbitrarily fast speed of response can be achieved. These formulas are used to develop a procedure to design feedback controllers with feedforward or two parameter output feedback type for achieving time response specifications. For a minimum phase plant we show that arbitrary transient response specifications, namely one with independently specified overshoot and specified rise time or speed of response can be exactly attained.**

***Index Terms*—Characteristic ratios, generalized time constant, overshoot, transient response.**

I. Introduction

Feedback control system design has to deal with the following problems: 1) asymptotic tracking and disturbance rejection of classes of signals such as steps, ramps, sinusoidal inputs; 2) stability and robust stability; and 3) transient response control. The first two topics have received a great deal of attention. (see [1]–[3] and the references therein).

Manuscript received April 23, 2002; revised November 7, 2002, April 18, 2003, and August 25, 2003. Recommended by Associate Editor F. M. Callier. This research is supported in part by the National Science Foundation under Grant HRD-9706268 and by the National Aeronautics and Space Administration under Grant NCC-5228. This research was done while Y. C. Kim was a Visiting Scholar at Tennessee State University, Nashville, TN.

Y. C. Kim is with the School of Electrical and Electronic Engineering, Chungbuk National University, Cheongju, Republic of Korea.

L. H. Keel is with the Center of Excellence in Information Systems, Tennessee State University, Nashville, TN 37203-23401 USA.

S. P. Bhattacharyya is with the Department of Electrical Engineering, Texas A&M University, College Station, TX 77843 USA.

Digital Object Identifier 10.1109/TAC.2003.820153

On the other hand, there are very few results dealing with the problem of transient response control, despite the fact that good transient response is one of the most important requirements for every control system. For a certain class of transfer functions whose poles are all real, negative, and distinct, analytical expressions of transient responses were provided in [4]. It was also shown that this formula in closed form can be used to determine the zeros that result in minimum transient time. In [5]–[7], some limitations on transient response are studied in terms of poles and zeros of the system. The ℓ_1 optimal control approach proposed in [8] specifically deals with the worst case time domain response under bounded amplitude inputs and is one of few "modern" approaches to time response control (also see [9] for other optimization based approaches). Based on asymptotic time scale and eigenstructure assignment, a solution to a robust perfect tracking problem for minimum phase multiple-input–multiple-output systems in the presence of initial conditions and external disturbances has been reported in [10]. In [11] and [12], the relationship of undershooting step responses and nonminimum phase zeroes has been studied, and in [13] and [14] the design of nonovershooting controllers for discrete time systems have been proposed. A good summary of classical control approaches can be found in [15] and [16].

This note presents some new results to directly address the transient response control problem. The main ideas are based on certain relations between characteristic polynomial coefficients and time domain responses. These relations were initially presented by Naslin in the 1960s [17]. An important contribution in this regard is due to Manabe [18] who investigated the problem of obtaining good transient response in control systems. His investigation focused on studying the generic behavior of the plant in the context of the so-called coefficient diagram that depicts the coefficients of the plant and characteristic polynomial on a logarithmic scale. Using this diagram, he successfully designed controllers for many industrial systems.

In this note, we begin by defining two important sets of parameters called here *generalized time constant* and *characteristic ratios*, respectively. These parameters are written in terms of coefficients of a polynomial. The properties of these parameters with respect to time domain response, in particular speed of response and overshoot, are then derived analytically. These properties are later used to construct a desired transfer function and a controller design procedure for minimum phase plants to achieve a transient response, with *independently* specified overshoot and rise time. The controller can be of state feedback plus feedforward or of two parameter type. The same procedure can be used for non minimum phase systems where reduced overshoot and increased speed of response may be obtained although they may not be independently specifiable.

II. Step Response Speed-Up

In this section, we develop some preliminary results on "speeding up" (or "slowing down") the step response of a system. If $x(t)$ is a signal $w(t) = x(\beta t)$ is a time scaled version of $x(t)$ and is speeded up if $\beta > 1$ and slowed down if $0 < \beta < 1$.

Let $y(t)$ denote the forced response, to a step $r(t)$, of a system with transfer function $G(s)$. We are interested in determining a system with transfer function $H(s)$ so that its forced response to $r(t)$ is $y(\beta t)$ for a given $\beta > 0$. We say that $H(s)$ speeds up the step response of $G(s)$ by a factor β. Let

$$G(s) = \frac{N(s)}{D(s)} = \frac{n_m s^m + n_{m-1} s^{m-1} + \cdots + n_1 s + n_0}{d_n s^n + d_{n-1} s^{n-1} + \cdots + d_1 s + d_0} = \frac{K(s - z_1)(s - z_2) \cdots (s - z_m)}{(s - p_1)(s - p_2) \cdots (s - p_n)} \quad (1)$$